Hindawi
Journal of Healthcare Engineering
Volume 2023, Article ID 9874046, 1 page
https://doi.org/10.1155/2023/9874046

Retraction

Retracted: Observation on the Effect of Intelligent Machine-Assisted Surgery and Perioperative Nursing

Journal of Healthcare Engineering

Received 15 August 2023; Accepted 15 August 2023; Published 16 August 2023

This article has been retracted by Hindawi following an investigation undertaken by the publisher [1]. This investigation has uncovered evidence of one or more of the following indicators of systematic manipulation of the publication process:

(1) Discrepancies in scope
(2) Discrepancies in the description of the research reported
(3) Discrepancies between the availability of data and the research described
(4) Inappropriate citations
(5) Incoherent, meaningless and/or irrelevant content included in the article
(6) Peer-review manipulation

The presence of these indicators undermines our confidence in the integrity of the article's content and we cannot, therefore, vouch for its reliability. Please note that this notice is intended solely to alert readers that the content of this article is unreliable. We have not investigated whether authors were aware of or involved in the systematic manipulation of the publication process.

In addition, our investigation has also shown that one or more of the following human-subject reporting requirements has not been met in this article: ethical approval by an Institutional Review Board (IRB) committee or equivalent, patient/participant consent to participate, and/or agreement to publish patient/participant details (where relevant).

Wiley and Hindawi regrets that the usual quality checks did not identify these issues before publication and have since put additional measures in place to safeguard research integrity.

We wish to credit our own Research Integrity and Research Publishing teams and anonymous and named external researchers and research integrity experts for contributing to this investigation.

The corresponding author, as the representative of all authors, has been given the opportunity to register their agreement or disagreement to this retraction. We have kept a record of any response received.

References

[1] L. Lei, "Observation on the Effect of Intelligent Machine-Assisted Surgery and Perioperative Nursing," *Journal of Healthcare Engineering*, vol. 2022, Article ID 6264441, 12 pages, 2022.

Hindawi
Journal of Healthcare Engineering
Volume 2022, Article ID 6264441, 12 pages
https://doi.org/10.1155/2022/6264441

Research Article

Observation on the Effect of Intelligent Machine-Assisted Surgery and Perioperative Nursing

Liping Lei

Operating Room, The Second Affiliated Hospital of University of South China, Hengyang 421001, Hunan, China

Correspondence should be addressed to Liping Lei; 14111822201@stu.wzu.edu.cn

Received 6 January 2022; Revised 24 January 2022; Accepted 31 January 2022; Published 21 March 2022

Academic Editor: Bhagyaveni M.A

Orthopedic surgery and care during the perioperative period are the key to the treatment of orthopedic diseases, which can quickly and effectively treat orthopedic diseases and can quickly recover during the perioperative period. Therefore, this paper focuses on the observation of the effect of intelligent machine-assisted surgery and perioperative care, combined with smart wearable devices and C-arm camera calibration; the details of the bone surgery are assisted by the machine, and then the recognition ability is accelerated by writing into the digital bone bank. Based on machine vision, CNN training and learning are designed to design a machine-assisted perioperative nursing method. This paper also designed a bone surgery test experiment and perioperative adverse event data analysis, combined with the data obtained from the experiment, designed a comparison experiment with traditional surgery and perioperative nursing. The experimental results show that the success rate of machine-assisted surgery is increased by nearly 2%–15% compared with traditional surgery; and the rehabilitation degree of machine-assisted perioperative nursing is 15.83% higher than that of traditional perioperative nursing.

1. Introduction

With the aging of society, the shortage of talents, and the increase of personnel expenses, the development of intelligent nursing robots is expected to have extensive development. The action recognition technology of nursing objects is an important research content of intelligent nursing robots. There are many types of plastic surgery diseases, and surgery is also difficult. The computer-assisted plastic surgery system combines computer technology, image processing technology, and medical knowledge to effectively support clinical surgery, improve the safety and success rate of surgery, and support plastic surgeons. It can be seen from this that the smooth resolution of intractable diseases has become a major innovation in the traditional surgical model.

Robot-assisted plastic surgery is the current research hotspot in the field of plastic surgery. This is to protect doctors and patients, reduce X-ray damage, improve surgical positioning accuracy, and reduce surgical operations. It is a typical combination of medical technology and industrial technology. At the same time, as a new technology of digital plastic surgery, it provides digital models of allografts and artificial bones, realizes parameter measurement of three-dimensional anatomical models, saves and manages information related to surgery, and has unique advantages. In order to better meet the accuracy and safety requirements of plastic surgery, virtual surgery simulation, digital human bone model library, and the establishment of a computer-assisted plastic surgery system for digital models of allografts and artificial bones have become a top priority.

The innovation of this paper lies in the use of smart wearable devices combined with C-arm camera calibration and then access to the digital bone bank to achieve rapid identification and precise repair of injury sites in orthopedic surgery. Then use machine vision sensors for CNN training and learning, and then write perioperative DVT risks, so that perioperative care can be treated quickly and effectively, and patients can quickly recover.

2. Related Work

The Bionic Micro Suction Cup (mSC) is designed for patient-friendly smart medical skin drying adhesives. The

powerful Van der Waals force and induced negative pressure generated by the super soft mSC promote tight skin coupling without causing discomfort or irritation. Choi et al. found that it improves the sensitivity of embedded retractable electronic devices to continuous vital signs monitoring and can monitor vital signs without losing stickiness [1]. He uses a bionic microsuction cup to assist in the treatment of dry skin in medical applications, which has a certain reference value in machine-assisted treatment. In order to study the application of smart phone apps in medical treatment, Sayedalamin et al. discussed the practicality, attitudes, and trends of medical students at King Abdulaziz University (KAU) in Jeddah (SA), Saudi Arabia, towards smartphone-related medical applications (Apps), and their views on the impact of medical applications in training activities [2]. The medical services he studied are not very useful in society as a whole. With the advancement of medical technology based on multimedia and pattern recognition, smart medical treatment and individual smart medical treatment in smart hospitals, such as disease diagnosis, health monitoring, etc., play an important role in the life of this paper. Jiang et al. studied the energy-saving multicast routing problem in multihop wireless networks for these medical applications [3]. He is studying the energy-saving problem of wireless networks, but this paper mainly studies the application of machine-assisted medical care. In order to evaluate the feasibility, safety, and usefulness of augmented reality assisted urological surgery using smart glasses (SG), Borgmann et al. use technical metadata (number of photos taken/number of videos recorded/time of video recorded) and structured interviews with urologists using SG to assess feasibility. Safety is assessed by recording complications and grading according to the Clavien-Dindo classification [4].

What he studied is the feasibility and safety of smart glasses-assisted urological surgery, which has great reference value for this paper. This paper mainly studies the feasibility of machine-assisted surgery. The latest development of wearable electronic devices has promoted the research of new materials, sensors, and microelectronics technology to realize devices with higher functions and performance. Kassanos et al. outline new designs, embodiments, manufacturing methods, instrumentation, and informatics, as well as the challenges of developing and deploying such devices and clinical applications that can benefit from them. He emphasized the need and use of these technologies in the perioperative surgical care approach and the vision for the future and how potential end users and healthcare systems can adopt these tools [5]. The use of wearable devices in medical surgery is a problem worthy of attention. This paper mainly studies machine-assisted medical surgery. The approach for accelerated recovery after surgery (ERAS) is related to the improvement of perioperative results after several surgical procedures. Page et al. prospectively develop and implement evidence-based and standardized perioperative care approaches for patients undergoing open liver surgery. For patients undergoing surgery before and after the introduction of the ERAS pathway, an online questionnaire was used to assess the provider's views on the perioperative pathway [6].

The collected views of patients during the perioperative period are of great help to the perioperative care of this paper, but the main research is open liver surgery, while the main research of this paper is surgery. Contrary to the intraoperative period, it is well known that the current perioperative environment is fragmented and expensive. One of the potential solutions to this problem is that the Perioperative Surgery Home (PSH) care model proposed by Desebbe et al. is a patient-centered microhealth care system that starts when the surgical decision is made, runs through the entire perioperative period, and ends 30 days after discharge from the hospital [7]. The PSH researched by him has great reference value for this paper, and it would be more in line with the purpose of this paper if it can be added to machine assistance. Pancreaticoduodenectomy (PD) is the only possible cure for pancreatic cancer, and enhanced postoperative recovery (ERAS) evidence-based guidelines for PD perioperative care can be used to reduce changes in practice. The main purpose of Aviles et al. is to evaluate the feasibility of ERAS guidelines for PD patients [8].

3. Machine-Assisted Surgery and Perioperative Nursing Methods

3.1. Surgical Operations Based on Wearable Devices

3.1.1. Smart Wearable Devices. Smart wearable devices [9] are smart designs for everyday clothing and accessories such as smart bracelets, smart watches, and smart glasses. Specifically, it is a high-tech machine that can be installed on the body. Generally, these devices can integrate advanced technologies such as multimedia, wireless communication, sensors, virtual reality, flexible screens, GPS positioning systems, and biometrics. This is the integration of traditional hardware equipment and mobile Internet technology, which helps modern people provide more comfortable and convenient life tools.

Virtual reality technology [10] has developed rapidly in recent years and is a technology associated with many technologies. Using the latest high-tech with computer technology as the core, it generates actual visual, sound, and tactile virtual environments within a specific range. Objects in equipment and virtual environments "computers have evolved from initial numerical calculations to the processing of various media information such as text, images, and sound. Multimedia information is now used in virtual reality systems." The method of interaction between humans and computers in virtual reality is the use of computers for interacting with interface devices such as monitors, keyboards, and mice. Learning how to operate the user's machine requires the use of voice recognition, motion recognition, and other technologies to enable users to use the most natural means to talk to the "environment" as the most formal method of dialogue.

Virtual reality headset is a device designed to implement virtual reality technology. It is a brand-new technology of the latest display technology and a very important application in extended reality, virtual reality, and stereo display. Compared with traditional displays, the display of virtual reality

equipment is small and effective, and its appearance is usually represented by the shape of a helmet or diving glass, which provides hardware and software technical guarantees for the realization of ant technology, let consumers enjoy the advantages of virtual reality technology as easily as possible through virtual reality headsets. Headphones can make product components more closely fit through reasonable matching of electronic equipment, cleverly designed optical models, and installation equipment. Virtual reality headsets can provide consumers with a virtual reality experience and provide the equipment needed to implement real technologies. Figure 1 shows 4 types of headsets.

3.1.2. C-Arm Camera Calibration. The surgical navigation system based on the C-arm X-ray machine [11] needs to display the graphics of the surgical tools in real-time and intuitively on the patient's fluoroscopy image [12].

Camera calibration is one of the basic techniques in machine vision research. The goal is to determine the mapping parameters from a three-dimensional scene to a two-dimensional image [13]. These parameters can be divided into internal parameters representing the inherent properties of the camera and external parameters representing the external properties of the camera. The internal parameters include the optical characteristic parameters and geometric parameters of the camera, and the external parameters refer to the pause parameters of the camera in the world coordinate system.

In the surgical navigation system based on the C-manipulator, the main work of camera calibration is to construct a projection model from the 3D influence part of the space to the 2D image and to solve the transformation mapping parameters from 3D to 2D.

In the field of machine vision research, the camera model can actually be regarded as the projection relationship from the actual point in the space to the corresponding point of the image. The pinhole projection method is the center projection method, which is an ideal projection model. The pinhole model [14] assumes that the linear propagation condition of light is used, and the light reflected from the surface of the object is projected onto the image plane through a small hole. The main components of the pinhole model are the optical center (projection center), imaging surfing, optical axis, etc., as shown in Figure 2.

3.1.3. Digital Ossuary. The database [15] is a set of interconnected data composed of a specific structure and reasonably stored in a computer storage device. High sharing, low redundancy, easy to expand data structure, high independence, data acquisition, addition, deletion, change, maintenance, communication with each other by own software to meet user requirements define the relationship between data elements and access various data in a timely manner. In medicine, database technology is introduced to organize medical data and models with the least storage space and the most reasonable structure [13]. Safe access technology better protects patient privacy, realizes the transfer and sharing of resources between different medical units, more extensively integrates various information on the Internet, and quickly and accurately retrieves target data sources, which brings great convenience to doctors and the entire medical work.

The digital bone bank [16] is an important part of the medical database. As a clinical application database, the overall design idea of the digital bone bank is to fully understand the overall framework of the system, take a top-down approach, and determine the specific requirements and relationships of each module in turn. The overall design of the digital ossuary is generally considered from the following two aspects:

(1) The Overall Design of the Technical Level. Clarifying the application goals of the database, list all the functions that need to be implemented, the required medical data, and the relationships between the various modules. Since it is not safe to modify specific internal units, and there is the possibility of changing the whole body, the preliminary planning should be done carefully.

(2) Overall Design at the Application Level. The clinical application database involves a wide range of information, many types, and great differences. This paper divides the data into two types: qualitative and quantitative. Qualitative data is expressed by "presence or absence," "positive and negative" or degree classification; quantitative data can generally be expressed with precise numerical values. There are dynamic and static differences between the two types of data. Static data remains the same for life. On the contrary, dynamic data changes in a few hours or even minutes will have a significant impact on the operation. The data type consists of text, image graphics, and indescribable information. Developers can only use careful planning and analysis to make application software that meets the requirements of orthopedic physicians as much as possible within the scope of the existing technology. The structure of the database system is shown in Figure 3.

The participation and suggestions of orthopedic physicians have important guiding significance for the development of a digital bone bank. The thinking modes of engineering and medicine are not the same, and software developers do not understand medicine. Only by constantly communicating and clarifying doctors' ideas and requirements can they design reasonable application software. Before it is put into production, the user experience of doctors is repeatedly collected and continuously improved so that the database software can finally be accepted and recognized by users [17].

3.2. Perioperative Care Based on Machine Vision

3.2.1. Machine Vision. Machine vision [18] has many fields, and its research content is very rich, including image processing, signal processing, optics, machinery, automation, electrical, computer software systems, robotics, and other fields. Machine vision began in the 1950s. At that time, only the recognition and acquisition of two-dimensional image features such as the character recognition of the license board, the two-dimensional

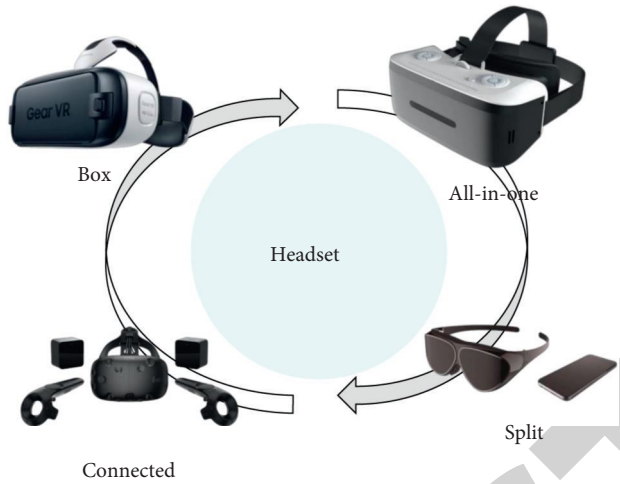

Figure 1: Virtual reality headset.

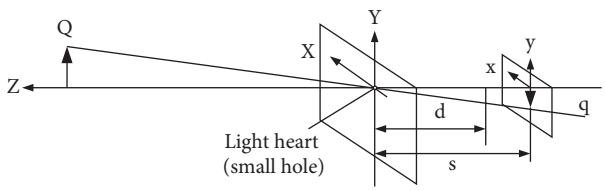

Figure 2: Pinhole camera model.

detection of the working size, the medical image processing, and the remote sensing image can be processed and analyzed.

Machine Vision plays an irreplaceable role in the fields of industry, economy, scientific research, and national defense. The machine vision system has the advantage of not directly contacting the measured object [19], so the possibility of mutual damage between the measuring instrument and the measured object after contact will be reduced. Moreover, the visual range of machine vision far exceeds the visual range of humans. Machine vision can use not only visible light for inspection but also use infrared, microwave, and ultrasonic for measurement. In addition, compared with manual inspection, machine vision systems have important advantages. In other words, machine vision runs for a long time in a harsh environment and has stable detection accuracy and stability. Figure 4 shows the application of machine vision.

However, machine vision also has some problems. For example, in many cases, machine vision has higher requirements for ambient light sources, which limits the application scope of some methods. Some machine vision methods are too computationally expensive, and even parallel computing techniques cannot meet the demand, which limits the speed of detection, the strict requirements of detection accuracy. At present, the accuracy of many industrial inspections is converted into pixel accuracy as subpixel accuracy. At present, the accuracy of many inspection algorithms is still maintained at pixel accuracy. In order to obtain a higher-precision ruler, sometimes other high-precision tools, such as gratings, are needed. Although machine vision can solve problems in many industrial fields, there is also a big gap that can replace humans in certain fields.

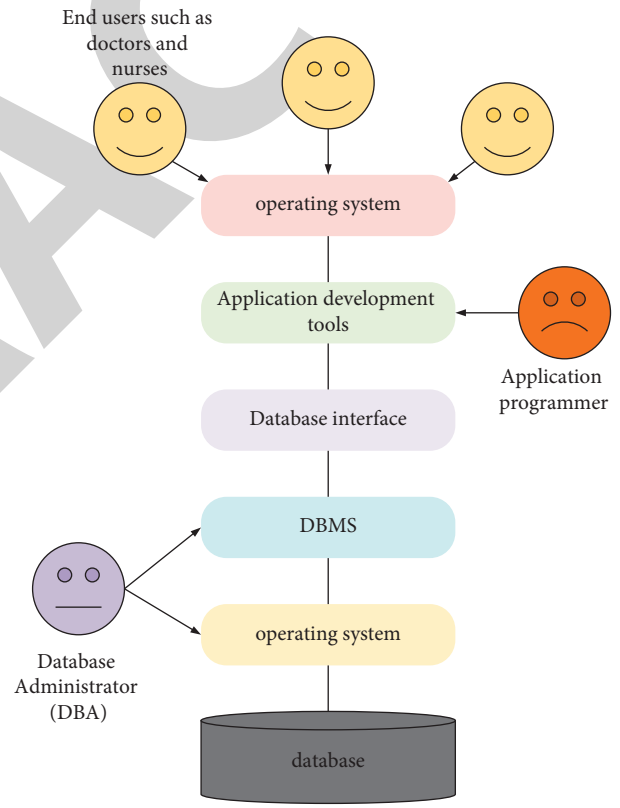

Figure 3: Database system structure diagram.

3.2.2. CNN Training and Learning. The cross-layer CNN-SVM model [20] proposed in this paper needs to train the feature extraction model CNN before performing the task. According to the characteristics of the cross-layer structure, the commonly used neural network training method-back propagation algorithm is improved, and a training algorithm suitable for the cross-layer CNN in this paper is designed [21]. Figure 5 shows the structure of CNN.

By inputting the behavior sample video, using the error between the output vector and the reference vector to correct the parameters in the calculation process achieves the

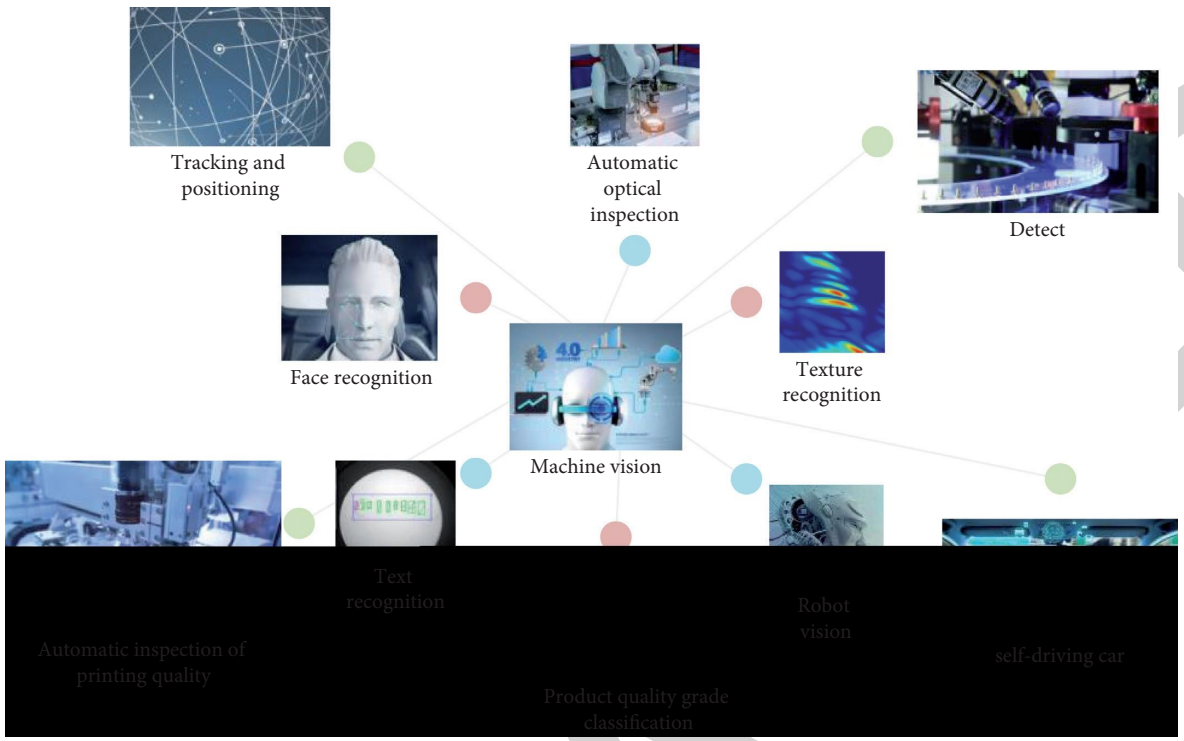

Figure 4: Application of machine vision.

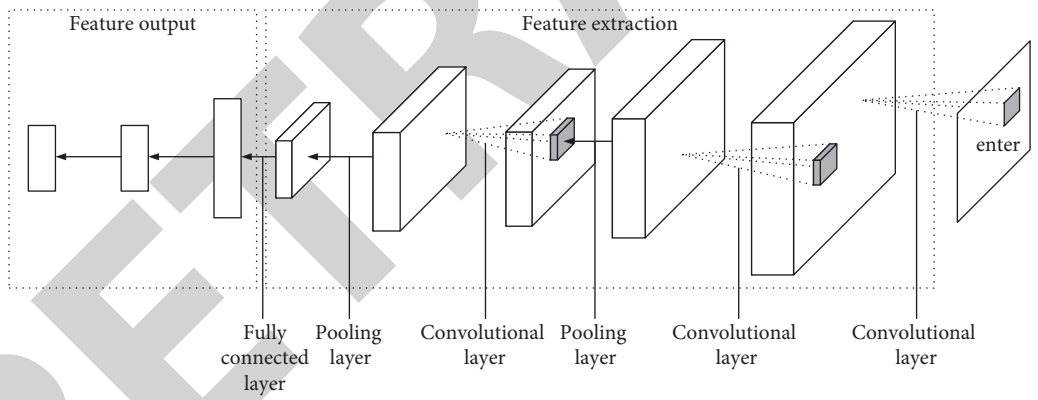

Figure 5: CNN structure.

purpose of reducing the output error. Supposing there are K training samples (a, b), the input of the network is recorded as a, the expected output is recorded as b, and the actual output is recorded as o. The objective function Q_K is defined as the mean square error of all samples. The calculation formula is as follows:

$$Q_K = \frac{1}{2}\sum_{N=1}^{K}\sum_{n=1}^{k}(o_n - b_n)^2. \tag{1}$$

Since the output layer and the upper layer neurons are completely connected, the error of the output layer is equal to the difference between the actual output and the expected output plus the partial derivative function of the activation function of the input vector. The calculation formula is as follows:

$$\theta_n^{(6)} = (o_n - b_n)\cdot f'\left(v_n^{(6)}\right). \tag{2}$$

The error of the fully connected layer F_5 is $(\theta^{(6)}_{n(1,2,3,\ldots,6)}, \theta^{(4)}_{n(1,2,3,\ldots,12)})$, and the calculation formula is as follows:

$$\theta_n^{(5)} = (R)^S\theta_n^{(6)}\cdot F_n^{(6)}\cdot\left(1 - F_n^{(5)}\right). \tag{3}$$

In which, $\theta^{(2)}_{n,m}$ represents the feedback transmission error of the m-th sampling feature map from the F_5 layer to the S_2 layer, and $\theta^{(4)}_{n,m}$ represents the feedback transmission error of the m-th sampling feature map from the F_5 layer to the S_4 layer.

The upsampling function is defined as follows:

$$vp_{\gamma\times\varphi}(a) = a \otimes 1_{\gamma\times\varphi}. \tag{4}$$

In which, $\gamma \times \varphi$ is the multiple factor for downsampling, $1_{\gamma\times\varphi}$ is a matrix with a size of $\gamma \times \varphi$ and an element value of 1, and "⊗" represents the Kronecker product internal filling operation. The error calculation formula of the convolutional layer C_3 is as follows:

$$\theta_{n,m}^{(3)} = \frac{1}{\gamma \times \varphi}\left(f'\left(v_{n,m}^{(3)}\right)\right) \cdot vp_{\gamma\times\varphi}\left(\theta_{n,m}^{(4)}\right), \quad 1 \le m \le 12. \tag{5}$$

Because the downsampling layer S_2 is connected to the downsampling layer S_4 and the fully connected layer F_5 at the same time, the error of S_2 is equal to the sum of the errors of the S_4 layer and the F_5 layer. The calculation formula is as follows:

$$\begin{aligned} \theta_{n,m}^{(2)} &= \theta_{n,m}^{(2)_1} + \theta_{n,m}^{(2)_2}, \\ \theta_{n,m}^{(2)_2} &= \left(\theta_{n,m}^{(3)} * i_{n,m}^{(3)}\right) \cdot f'\left(v_{n,m}^{(2)}\right), \quad 1 \le m \le 12. \end{aligned} \tag{6}$$

Or it is expressed as follows:

$$\theta_{n,m}^{(2)_2} = f'\left(v_{n,m}^{(2)}\right).\mathrm{conv2}\left(\theta_{n,m}^{(3)}, \mathrm{rot}\,180\left(i_{n,m}^{(3)}\right), \text{'full'}\right). \tag{7}$$

Like C_3, the error calculation formula of the convolutional layer C_1 is as follows:

$$\theta_{n,m}^{(1)} = \frac{1}{\gamma \times \varphi}\left(f'\left(v_{n,m}^{(2)}\right) \cdot vp_{\gamma\times\varphi}\left(\theta_{n,m}^{(1)}\right)\right), \quad 1 \le m \le 6. \tag{8}$$

After obtaining the feedback transmission error of each layer, the weighted deviation function and the bias deflection function are solved. Because the calculation method of downsampling is simplified, only the convolutional layer and the output layer need to be calculated.

Output layer:

$$\begin{aligned} \frac{\partial Q_K}{\partial W^{(6)}} &= \sum_{n=1}^{K}\left(\theta_n^{(6)}\right)^S F_n^{(5)}, \\ \frac{\partial Q_K}{\partial y^{(6)}} &= \sum_{n=1}^{K}\theta_n^{(6)}. \end{aligned} \tag{9}$$

C_3 layer:

$$\begin{aligned} \frac{\partial Q_K}{\partial i_{n,m}^{(3)}} &= \sum_{n=1}^{K} S_{n,m}^{(2)} * \theta_n^{(6)}, \\ \frac{\partial Q_K}{\partial y_m^{(3)}} &= \sum_{n=1}^{K}\theta_{n,m}^{(3)}. \end{aligned} \tag{10}$$

C_1 layer:

$$\begin{aligned} \frac{\partial Q_K}{\partial i_{n,m}^{(1)}} &= \sum_{n=1}^{K} a_n * \theta_{n,m}^{(1)}, \\ \frac{\partial Q_K}{\partial y_m^{(1)}} &= \sum_{n=1}^{K}\theta_{n,m}^{(1)}. \end{aligned} \tag{11}$$

Finally, the gradient descent method is used to modify the parameters. In summary, the specific training steps of the network are as follows:

Step 1. initializing the network, define $\Delta W = 0$, $\Delta i = 0$, $\Delta y = 0$;

Step 2. for the sample $n = 1 : K$,

(a) For the forward propagation process, use the forward propagation formula to calculate the activation value of the neurons in each layer of CNN;

(b) Calculating the error $\theta_n^{(6)}$ between the output data and the sample data for the CNN output layer;

(c) Calculating the feedback transmission error $(\theta_n^{(1)}, \theta_n^{(2)}, \ldots, \theta_n^{(5)})$ of each layer;

(d) Calculating the partial derivative $\partial Q_K/\partial W, \partial Q_K/\partial i, \partial Q_K/\partial y$ of the weight and bias of the network;

(e) Calculating

$$\begin{aligned} \Delta W^{(1)} &= \Delta W^{(1)} + \frac{\partial Q_K}{\partial W^1}, \\ \Delta i^{(1)} &= \Delta i^{(1)} + \frac{\partial Q_K}{\partial i^1}, \\ \Delta y^{(1)} &= \Delta y^{(1)} + \frac{\partial Q_K}{\partial y^1}. \end{aligned} \tag{12}$$

Step 3. update the weights and bias parameters; μ is the learning rate:

$$\begin{aligned} W^{(1)} &= W^{(1)} - \mu\left[\frac{1}{K}\right]\Delta W^{(1)}, \\ i^{(1)} &= i^{(1)} - \mu\left[\frac{1}{K}\right]\Delta i^{(1)}, \\ y^{(1)} &= y^{(1)} - \mu\left[\frac{1}{K}\right]\Delta y^{(1)}. \end{aligned} \tag{13}$$

Step 4. repeat the above steps to reduce the error until the error meets the requirements;

Step 5. the iteration stops.

3.2.3. DVT Risk during Perioperative Period. DVT [22] is a common complication in orthopedics clinics. Clinical studies have shown that during the entire perioperative period if effective DVT preventive measures are not taken, the incidence of DVT will be as high as 66.67%. Whether it is before, during or after surgery, patients have a higher incidence of DVT. At the same time, the harm of DVT has been unanimously agreed in the world. During the entire perioperative period, before DVT occurs, if we can screen high-risk patients with DVT, and if we can have a certain understanding of the development and changes of DVT during the orthopedic perioperative period, in clinical work, individualized and staged DVT prevention can be given to patients at different periods of the perioperative period

[23, 24]. Figure 6 shows the etiology and clinical manifestations of DVT.

With the aging of the domestic population, the number of elderly patients with hip fractures, especially femoral neck fractures, is increasing [25]. For elderly patients with femoral neck fractures older than 60 years, artificial hip replacement is the current mainstream treatment. Especially for elderly patients who are healthy and have a long life expectancy, artificial total hip joints are the main choice [26–28]. However, due to the many basic diseases of the elderly, the recovery of physical functions after trauma and surgery is slower than that of young people, and the overall incidence of complications during the perioperative period is significantly higher than that of young patients. According to foreign literature reports, the incidence of DVT in patients with femoral joint fractures within 24 hours after injury is 2.6%. If interventional therapy is not received to prevent thrombosis within 72 hours after injury, the incidence may increase to 13.3%. If DVT occurs, it may have a serious impact on the patient's life and quality of life and increase the patient's hospitalization time and hospitalization costs. It is important to screen the treatment methods for high-risk DVT patients and take timely preventive measures. Based on this, this study conducted TCM syndrome differentiation, DVT risk assessment, and TEG detection in elderly patients throughout the perioperative period to explore the characteristics of TCM syndrome, DVT risk, and blood coagulation status of patients during the perioperative period, to provide certain ideas and methods for the screening of patients with a high risk of DVT, to provide guidance for Chinese and Western prevention of DVT during the orthopedic perioperative period, and to improve the accuracy of prevention of DVT.

4. Machine-Assisted Surgery and Perioperative Nursing Experiment

4.1. Data Analysis of Adverse Events during Perioperative Period. A total of 57 adverse care events occurred in the samples selected in this paper. Among them, the incidence of defects in the injection of medicines, loss of surgical specimens, or improper preservation of bedsores was higher, which were 28.07%, 26.32%, and 10.53, respectively, as shown in Table 1. In addition, according to the classification criteria of the Hospital Authority on adverse events in nursing, 33 cases (57.89%) were classified as class 0, and 12 cases were classified as class I (21.5%), 10 cases were classified as class II (17.54%), 2 cases were classified as class III (3.51%), and 0 cases were each classified as class V.

The main reasons for 57 operating room-related adverse events in the samples were incomplete evaluation, strict implementation failure of the inspection system, and equipment defects. The details are shown in Table 2. The attribute analysis results of the adverse events are shown in Table 3.

The study included 57 cases of nursing adverse events during plastic surgery, including 11 men and 29 women (male : female = 1.28 : 1), a total of 40 operating room nurses. The youngest is 22 years old and the oldest is 48 years old. The average age of the selected nurses was 29.04 ± 5.67 years old. Of these, 29 have a university degree and 11 have a bachelor's degree or above. Among them, 60% of nurses have 0 to 5 years of work experience, 25% of nurses have 5 to 10 years of work experience, and 15% of nurses have more than 10 years of work experience. There are statistically significant differences among operating room nurses in different working years, such as bedsores, defects of infusion medicine, loss of surgical specimens, improper preservation, and other adverse events ($P < 0.05$). There is no statistical difference in the occurrence, which means that the academic qualification certificate will not affect the occurrence of adverse events, and the number of labor years will affect the occurrence of adverse events. The longer the working hours and the more experience, the lower the incidence of adverse events. Table 4 is the relationship between the occurrence of adverse nursing events in the operating room and the working years of the nurses. Table 5 displays the relationship between the occurrence of adverse nursing events in the operating room and the degree of nurses.

In the past 4 years, a total of 57 cases of adverse events during surgical care of plastic surgery patients were reported, with an incidence rate of 0.09%. Specimens are lost or improperly kept; compared with general wards, plastic surgery patients face complex and diverse care risks during surgery. This may be related to the complicated operating room environment, various instruments, heavy workload, and excessive work of nurses. This paper combines the characteristics of plastic surgery and develops and uses mechanical auxiliary nursing tools to avoid various adverse events.

4.2. Orthopedic Surgery Test Experiment. In the experiment, the corpse used was an individual scanned by CT. At the same time, the required reset force can be read by a force sensor mounted on the top of the parallel robot. Because the fixed needles will be displaced, the position of the fixed upper leg of the parallel robot and the bending Kjeldahl displacement is not equal to the relative displacement of the two broken bones. This site uses X-ray images to determine the relative displacement between broken bones. That is, after each parallel robot movement, X-rays are taken while reading the value of the force sensor. Next to the calf, a ruler containing steel balls at fixed intervals is placed in this paper so that the precise distance between the broken bones can be obtained in the X-ray picture.

As shown in Figure 7, the dotted line is the force position curve obtained through actual experiments, and the solid line is the force position curve obtained from the finite element model. The horizontal axis represents the distance between two broken tibias, and the vertical axis represents the traction required for this distance.

Part of the experimental data has changed, and the overall tilt has increased. From the knowledge of biomechanics, this is consistent with the laws of actual physiology. The muscles in the resting state are elastic and will stretch with external force. The greater the force, the greater the stretch. However, the longer the distance, the harder it is to

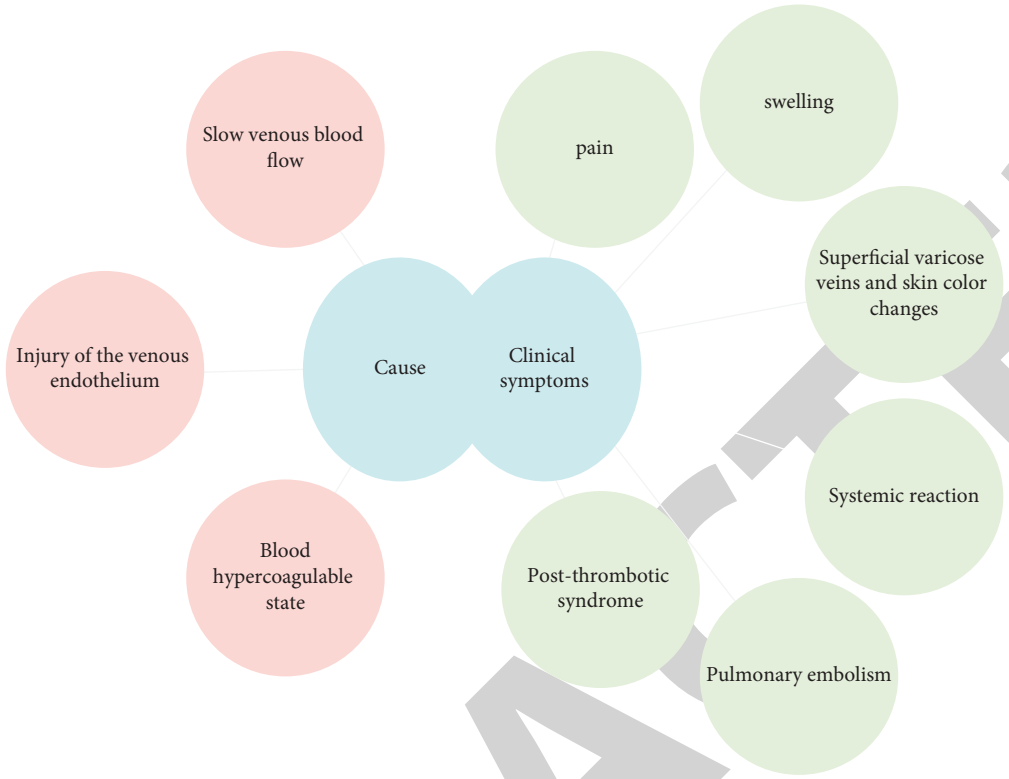

Figure 6: The etiology and clinical manifestations of DVT.

Table 1: Classification and classification of adverse events during the perioperative period.

Classification	Frequency	Classification of adverse nursing events				Total composition ratio (%)
		Level 0	Class I	Level II	Level III	
Pressure sore	16	12	4	0	0	28.07
Intraoperative infusion medication defects	15	10	2	3	0	26.32
Loss or improper storage of surgical specimens	6	1	5	0	0	10.53
Other accidents	5	5	0	0	0	8.77
Incision infection at the surgical site	4	0	0	4	0	7.02
Surgical items left in the body	3	1	1	1	0	5.26
Burns from electrosurgical equipment	2	1	0	1	0	3.51
Defects in nursing records	2	2	0	0	0	3.51
Orthostatic nerve injury	2	0	0	1	1	3.51
Wrong surgical site in surgical patients	1	1	0	0	0	1.75
Patient falls into bed	1	0	0	0	1	1.75
Total	57	33	12	10	2	100

Table 2: Distribution of the main causes of adverse events.

Reason	Frequency	Composition ratio (%)
Underassessment	14	24.56
Failure to strictly implement the verification system	13	22.81
Equipment and facilities medical supplies defects	9	15.79
Communication is not in place	8	14.04
Public accident	7	12.30
Patient's own disease factors	6	10.50
Summarize	57	100

Table 3: Statistics of "event attributes" of adverse events.

Category	Event attributes		Total
	Preventable (%)	Not preventable (%)	
Error event	27 (47.37%)	0 (0%)	27 (47.37%)
Accident	1 (1.75%)	4 (7.02%)	5 (8.77%)
Security incident	18 (31.58%)	1 (1.75%)	19 (3.33%)
Unpredictable events	3 (5.26%)	2 (3.51%)	5 (8.77%)
Communication event	1 (1.75%)	0 (0%)	1 (1.75%)
Complaint incident	0 (0%)	0 (0%)	0 (0%)
Total	50 (87.72%)	7 (12.28%)	57 (100%)

Table 4: The relationship between the occurrence of adverse nursing events in the operating room and the working years of the nurses.

Adverse events	Frequency	<5 years	5–10 years	>10 years	X^2	P
Pressure sore	16	14	1	1	8.156	0.016
Intraoperative infusion medication defects	15	13	1	0	6.829	0.027
Loss or improper storage of surgical specimens	6	5	1	0	1.261	0.567

Table 5: The relationship between the occurrence of adverse nursing events in the operating room and the degree of nurses.

Adverse events	Frequency	Education		X^2	P
		Junior college	Bachelor's degree and above		
Pressure sore	16	9	7	—	0.080
Intraoperative infusion medication defects	15	10	5	—	0.716
Loss or improper storage of surgical specimens	6	4	2	—	1.000

stretch, and the greater the tilt, as shown by the curve in Figure 8. The r curve represents the length-tension curve of the resting muscle, a represents the length-tension curve of the active muscle, and d represents the increased tension during stimulation.

It can be understood that local fluctuations are caused by the synthesis of multiple tendon tension length curves. When resisting traction, because the patient is anesthetized and loses consciousness, the muscles on the legs can be regarded as resting muscles. In the experimental data, the tension-displacement curve can be regarded as the synthesis of the tension-displacement curve of multiple static tendons of the leg.

The performance of the analog data is relatively flat, basically showing a linear trend. In the modeling and simulation of the leg model, whether it is the initial three-dimensional modeling or the later finite element modeling, many simplification schemes are used, and errors will inevitably occur. Example: in actual situations, the muscles do not follow the hook rule. If the muscles are stretched again, they will stretch easily. In other words, the curve is getting steeper and steeper, but the finite element model does not reflect this well.

Due to experimental errors and the simplification of the model, there are differences between the two data sets, but in general, the trends and values of the two data sets are very consistent. Especially in the usual clinical traction range of 2–8 mm, the effect can meet the needs of clinical simulation.

4.3. Respiration Compensation Experiment. Use the NDI optical tracking equipment to measure the real-time coordinates of the spine and the robot and then run an algorithm to solve the compensated position, move the robot to the compensated position, and get the relevant data. The description of the pose of a space object involves 6 degrees of freedom. Therefore, this paper chooses the way of describing the coordinate system to describe the space object, selects a reference point, and uses $p(x, y, z, qw, qx, qy, qz)$ to describe it. The first three elements represent the position, and the latter four elements represent the posture, expressed in the form of a quaternion. Inputting a periodic sine signal to the breathing simulation device, control the sampling interval to be set to 100 ms, collect data every other sampling interval, perform calculations, and drive related equipment to move to the compensation point. According to the experimental data obtained, this paper analyzes its error and accuracy, and the experimental data is processed by MATLAB software as shown in Figure 9.

By changing the amplitude and period of the sine motion of the breathing simulator and making it change, the stability of the compensation algorithm in this paper can be judged and evaluated. Finally, the relevant conclusions are drawn according to the error table: the displacement error is stable and not affected by the sinusoidal movement of the up and down movement device. That is, it has nothing to do with the change of the period and the amplitude. The maximum position error does not exceed 0.6 mm, which meets the experimental requirements of this paper. Since the system mainly moves in the z-axis direction, the maximum error appears in the z-direction. This control algorithm meets the needs of this paper.

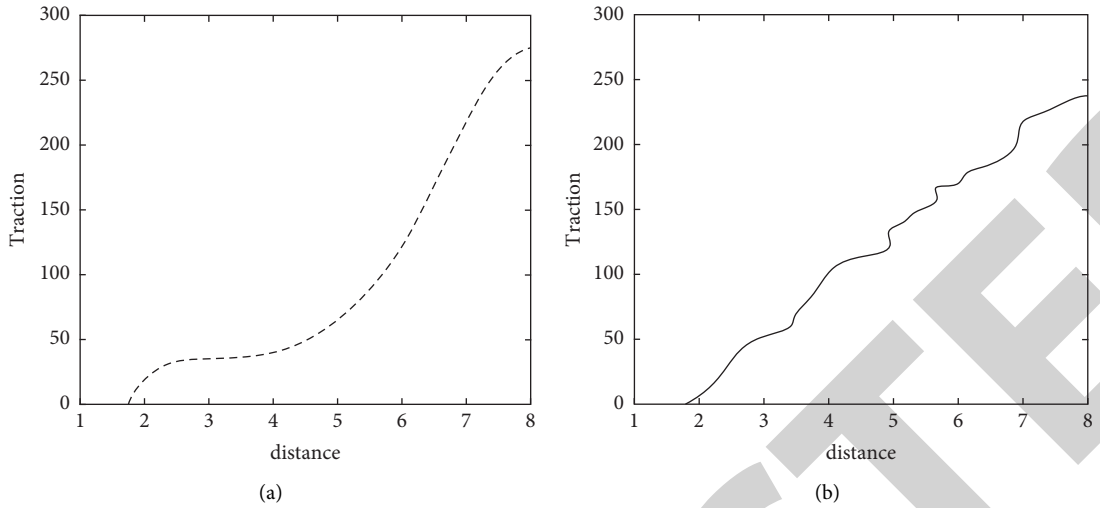

Figure 7: Two sets of data from experiment and finite element analysis, respectively. (a) Reduction surgery, (b) Finite element model.

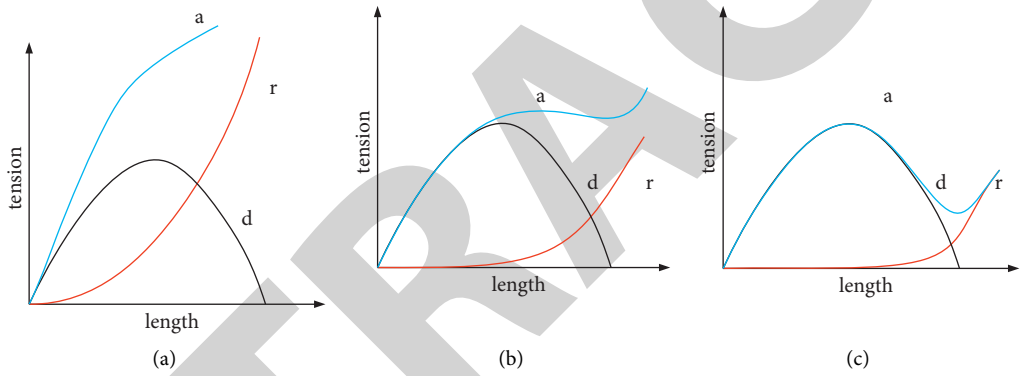

Figure 8: Tension-length curves of the three muscles. (a) Gastrocnemius muscle, (b) Sartorius muscle, (c) Semitendinosus muscle.

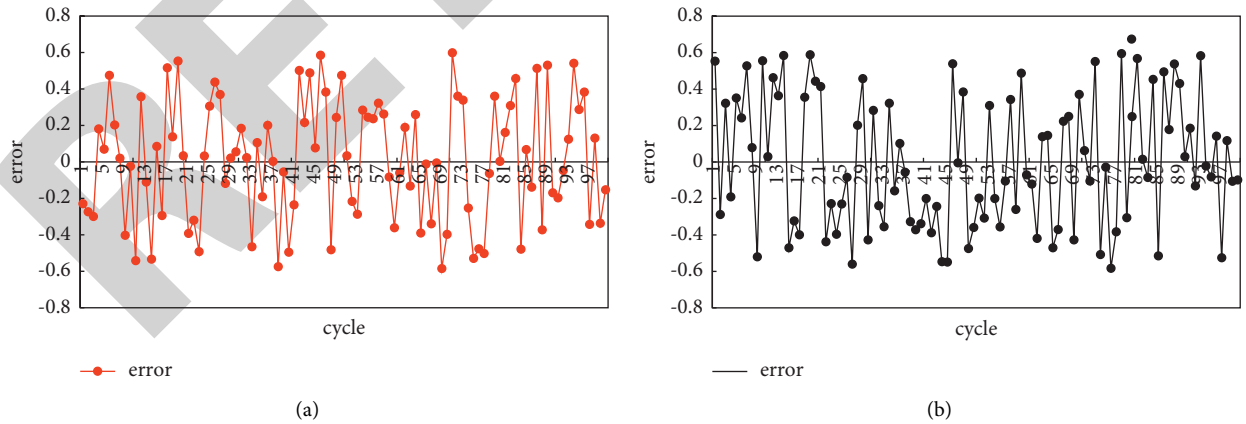

Figure 9: Rotation error image. (a) The first experiment. (b) The second experiment.

5. Results and Discussion

This paper analyzes the data obtained from the experiment and finally establishes a machine vision-based orthopedic surgery method and perioperative care. In order to explore the effect of its practical application, this paper sets up a comparative experiment with traditional surgery and nursing. The experiment is divided into an experimental group and a control group, and the experimental results are shown in Figure 10.

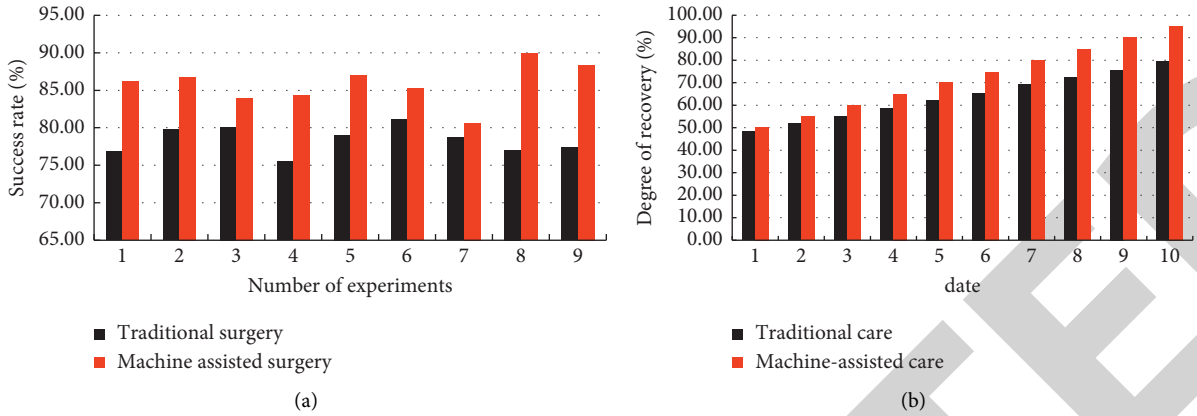

Figure 10: Comparison of experimental results based on machine-assisted surgical operation and perioperative nursing and traditional. (a) Surgical operation success rate. (b) Degree of nursing recovery during the perioperative period.

It can be seen from Figure 10 that the success rate of machine-assisted surgery and the degree of nursing rehabilitation during the perioperative period are significantly higher than that of traditional surgery. The success rate of machine-assisted surgery can reach 80%–90%, while the success rate of traditional surgery is only 75%–82%, an increase of nearly 2%–15%. The degree of nursing rehabilitation during the perioperative period reached 95.18% in 10 days, while the degree of rehabilitation in traditional nursing was only 79.35%, an increase of about 15.83%. This shows that machine-assisted surgery can increase the probability of successful surgery and speed up the degree of recovery during the perioperative period.

6. Conclusions

The main research in this paper is based on machine-assisted surgery and nursing during the perioperative period. In order to study the application of machine-assisted surgery, this paper mainly chooses orthopedic surgery as the main entry point. By combining wearable smart devices and C-arm camera calibration, a machine-assisted surgical operation mode is designed. Then, based on the establishment of a digital bone bank, the injured part of orthopedic surgery can be quickly located and then treated. During the perioperative period, this paper combines the intelligent sensors of machine vision after CNN training and learning and then writes the intelligent sensors into the DVT risk analysis. Perioperative care based on machine vision can effectively prevent various emergencies of patients and can achieve the effect of digital care through CNN training. This paper also designed a bone surgery test experiment and perioperative adverse event data analysis and then combined the experimental data to design a comparison experiment with traditional surgery and perioperative care. This shows that machine-assisted surgery and perioperative nursing can effectively improve the success rate of surgery and the degree of nursing recovery.

Data Availability

The data used to support the findings of this study are available from the author upon request.

Conflicts of Interest

The authors declare no conflict of interest.

Acknowledgments

The work was not supported by any funding.

References

[1] M. K. Choi, Ok K. Park, C. Choi et al., "Cephalopod-inspired miniaturized suction cups for smart medical skin," *Advanced Healthcare Materials*, vol. 5, no. 1, pp. 80–87, 2016.

[2] Z. Sayedalamin, A. Alshuaibi, O. Almutairi, M. Baghaffar, T. Jameel, and M. Baig, "Utilization of smart phones related medical applications among medical students at King Abdulaziz University, Jeddah: a cross-sectional study," *Journal of Infection and Public Health*, vol. 9, no. 6, pp. 691–697, 2016.

[3] D. Jiang, W. Li, and H. Lv, "An energy-efficient cooperative multicast routing in multi-hop wireless networks for smart medical applications," *Neurocomputing*, vol. 220, pp. 160–169, 2017.

[4] H. Borgmann, M. R. Socarrás, J. Salem et al., "Feasibility and safety of augmented reality-assisted urological surgery using smartglass," *World Journal of Urology*, vol. 35, no. 6, pp. 967–972, 2017.

[5] P. Kassanos, M. Berthelot, J. A. Kim, B. M. G. Rosa, F. Seichepine, and S. Anastasova, "Smart sensing for surgery: from tethered devices to wearables and implantables," *IEEE Systems, Man, and Cybernetics Magazine*, vol. 6, no. 3, pp. 39–48, 2020.

[6] A. J. Page, F. Gani, K. T. Crowley et al., "Patient outcomes and provider perceptions following implementation of a standardized perioperative care pathway for open liver resection," *Journal of British Surgery*, vol. 103, no. 5, pp. 564–571, 2016.

[7] O. Desebbe, T. Lanz, Z. Kain, and M. Cannesson, "The perioperative surgical home: an innovative, patient-centred and cost-effective perioperative care model," *Anaesthesia Critical Care & Pain Medicine*, vol. 35, no. 1, pp. 59–66, 2016.

[8] C. Aviles, M. Hockenberry, D. Vrochides et al., "Perioperative care implementation: evidence-based practice for patients with pancreaticoduodenectomy using the enhanced recovery

after surgery guidelines," *Clinical Journal of Oncology Nursing*, vol. 21, no. 4, pp. 466–472, 2017.

[9] T. Crossland, P. Stenetorp, S. Riedel, D. Kawata, T. D. Kitching, and upert A. C. Croft, "Towards machine-assisted meta-studies: the Hubble constant," *Monthly Notices of the Royal Astronomical Society*, vol. 492, no. 3, pp. 3217–3228, 2020.

[10] R. E. Austin, "Commentary on: patient satisfaction with an early smartphone-based cosmetic surgery postoperative follow-up," *Aesthetic Surgery Journal*, vol. 38, no. 1, pp. 110–113, 2018.

[11] J. T. Highsmith, D. A. Weinstein, M. J. Highsmith, and J. R. Etzkorn, "BIOPSY 1-2-3 in dermatologic surgery: improving smartphone use to avoid wrong-site surgery," *Technology & Innovation*, vol. 18, no. 2-3, pp. 203–206, 2016.

[12] K. Axel, "Smart robot performs vision-assisted surgery," *Vision Systems Design*, vol. 22, no. 5, pp. 15–18, 2017.

[13] G. A. Robertson, S. J. Wong, R. R. Brady, and A. S. Subramanian, "Smartphone apps for spinal surgery: is technology good or evil?" *European Spine Journal*, vol. 25, no. 5, pp. 1355–1362, 2016.

[14] C. J. Peden, G. Aggarwal, R. J. Aitken et al., "Guidelines for perioperative care for emergency laparotomy enhanced recovery after surgery (ERAS) society recommendations: Part 1—preoperative: diagnosis, rapid assessment and optimization," *World Journal of Surgery*, vol. 45, no. 5, pp. 1272–1290, 2021.

[15] I. O. Fleming, C. Garratt, R. Guha et al., "Aggregation of marginal gains in cardiac surgery: feasibility of a perioperative care bundle for enhanced recovery in cardiac surgical patients," *Journal of Cardiothoracic and Vascular Anesthesia*, vol. 30, no. 3, pp. 665–670, 2016.

[16] J. R. Datillo, D. J. Gittings, M. Sloan, W. Hardaker, M. Deasey, and N. Sheth, "Is there an app for that? orthopaedic patient preferences for A smartphone application," *Applied Clinical Informatics*, vol. 8, no. 3, pp. 832–844, 2017.

[17] C. Ngarambe, B. J. Smart, N. Nagarajan, and J. Rickard, "Validation of the Surgical Apgar Score after laparotomy at a tertiary referral hospital in Rwanda," *World Journal of Surgery*, vol. 41, no. 7, pp. 1734–1742, 2017.

[18] E. M. García, P. D. R. de Diego, C. T. de Las Heras, and P. C. Escudero, "Experience of a pediatric monographic hospital and strategies adopted for perioperative care during the SARS-CoV-2 epidemic and the reorganization of urgent pediatric care in the Community of Madrid, Spain," *Revista Espanola de Anestesiologia y Reanimacion*, vol. 67, no. 9, pp. 527-528, 2020.

[19] M. Charlesworth, B. G. Williams, and M. H. Buch, "Advances in transcatheter aortic valve implantation, part 2: perioperative care," *BJA Education*, vol. 21, no. 7, pp. 264–269, 2021.

[20] F. Jamil, "Smartphone photography in oral and maxillofacial surgery," *British Journal of Oral and Maxillofacial Surgery*, vol. 54, no. 1, pp. 104-105, 2016.

[21] M. R. Mathis, T. Z. Dubovoy, M. D. Caldwell, and M. C. Engoren, "Making sense of big data to improve perioperative care: learning health systems and the multicenter perioperative outcomes group," *Journal of Cardiothoracic and Vascular Anesthesia*, vol. 34, no. 3, pp. 582–585, 2020.

[22] A. Nikolic, P. S. Waters, O. Peacock et al., "Hybrid abdominal robotic approach with conventional transanal total mesorectal excision (TaTME) for rectal cancer: feasibility and outcomes from a single institution," *Journal of Robotic Surgery*, vol. 14, no. 4, pp. 633–641, 2020.

[23] H. Yu, Y. Zhao, Z. Liu et al., "Research on the financing income of supply chains based on an E-commerce platform," *Technological Forecasting and Social Change*, vol. 169, Article ID 120820, 2021.

[24] Z. Liu, L. Lang, L. Li, Y. Zhao, and L. Shi, "Evolutionary game analysis on the recycling strategy of household medical device enterprises under government dynamic rewards and punishments," *Mathematical Biosciences and Engineering*, vol. 18, no. 5, pp. 6434–6451, 2021.

[25] J. Chen, Q. Zou, and J. Li, "DeepM6ASeq-EL: prediction of human N6-methyladenosine (m6A) sites with LSTM and ensemble learning," *Frontiers of Computer Science*, vol. 16, no. 2, pp. 1–7.

[26] G. Briganti, M. Scutari, and P. Linkowski, "A machine learning approach to relationships among alexithymia components," *Psychiatria Danubina*, vol. 32, no. 1, pp. 180–187, 2020.

[27] B. Belkız Güngör, A. İkra Akgül, İ. Taymur, H. Demirci, and A. İnel, "Evaluation of eating attitudes, anger and impulsivity in atypical and non-atypical depression and assessment of comorbidity of binge eating," *Psychiatria Danubina*, vol. 32, no. 1, pp. 105–114, 2020.

[28] K. Mardiana-Jansar and M. M. Hanafiah, "Visual communication technique to enhance teaching and learning processes in quantitative analysis and instrumentation course," *Acta Informatica Malaysia (AIM)*, vol. 4, no. 1, pp. 7–9, 2020.